Synthesis, Properties, and Applications of Tetraphenylmethane-Based Molecular Materials for Light-Emitting Devices

Hsiu-Chih Yeh,[†] Rong-Ho Lee,[‡] Li-Hsin Chan,[†] Tzu-Yao Jeremy Lin,[†] Chin-Ti Chen,*[,†] Easwaramoorthy Balasubramaniam,[†] and Yu-Tai Tao[†]

Institute of Chemistry, Academia Sinica, Taipei, Taiwan 11529, Republic of China, Opto-Electronics & Systems Lab., Industrial Technology Research Institute, Chutung, Hsinchu, Taiwan 310, Republic of China

Received October 9, 2000. Revised Manuscript Received June 29, 2001

Tetraphenylmethane-based compounds, tetrakis(4-(5-(3,5-di-*tert*-butylphenyl)-2-oxadiazolyl)phenyl)methane (TBUOXD), tetrakis(4-(5-(3,4-dimethoxyphenyl)-2-oxadiazolyl)phenyl)methane (OMEOXD), tetrakis(4-(5-(3-(α,α,α-trifluoromethylphenyl))-2-oxadiazolyl)phenyl)-methane (CF3OXD), tetrakis(4-(5-(4-diphenylaminophenyl)-2-oxadiazolyl)phenyl)methane (*p*-TPAOXD), and tetrakis(3-(5-(4-diphenylaminophenyl)-2-oxadiazolyl)phenyl)methane (*m*-TPAOXD), were synthesized. These compounds were characterized by NMR, microanalysis, UV−visible spectroscopy, fluorescence spectroscopy, cyclic voltammetry, DSC, and TGA. TBUOXD**,** OMEOXD, and CF3OXD showed rather similar electrochemical and spectroscopic characteristics to those of the hole-blocking material 2-(4-biphenylyl)-5-(4-*tert*-butylphenyl)-1,3,4-oxadiazole (PBD). However, TBUOXD**,** OMEOXD, and CF3OXD all crystallize well above 200 °C, much higher than the 70−90 °C observed for PBD. In addition, high onset glass transition temperatures of 97−175 °C were detected for the compounds. Both CF3OXD and PBD were adopted as a hole-blocking layer in organic light-emitting devices (OLEDs). A comparable performance with an external quantum efficiency of ∼1% was obtained for devices based on both CF3OXD and PBD, although a much lower allowed current density was found for the CF3OXD-based device. The bipolar blue fluorescent isomers *p*-TPAOXD and *m*-TPAOXD are both amorphous, showing no melting and crystallization transition. Only glass transitions at 187 and 149 °C were observed respectively. Single-layer OLEDs based on these two compounds were also fabricated by varied fabrication conditions (solvent, cathode material, film thickness, polymer blending). A turn-on voltage as low as 4 V, blue electroluminescence with an intensity of 1700 cd/m^2, and a photometric efficiency more than 0.8 cd/A can be achieved with *p*-TPAOXD-based devices.

Introduction

Organic light-emitting diodes (OLEDs) have made rapid advances (in low turn-on voltage, luminescence intensity, operation lifetime, full color display capability, and reasonable power efficiency) recently and have appeared ready to enter the commercial stage in the flat-panel display market.[1] All prosperous research activities of OLEDs in recent years were first inspired by the high-efficiency, small-molecule-based, heterojunction OLEDs demonstrated by a Kodak research team in the late eighties.[2] The surge in OLED research was then intensified further in the early nineties when the Cambridge group reported the polymer (polyphenylenevinylene, PPV)-based OLEDs,[3] which are attractive due to the simplicity and low cost in fabrication in addition to the possible application for flexible displays.[4] Although significantly improving in recent years, polymer-based OLEDs with high performance are not as common as molecule-based OLEDs. This is mainly due to the fact that polymeric materials with high purity are not as readily available as are molecular materials.[1a,5] Aggregation (or crystallization) is a serious problem for molecular π-conjugated materials, which rarely show amorphous glass phases. The boundary of crystalline regions in either the emissive layer or the charge-transporting layer creates irregularities or "defects", which usually act as traps for mobile electrons or holes as they move past. Charges in such a trap generate no radiation but dissipate energy as heat or vibrations and thus adversely affect the performance of molecule-based OLEDs.[6]

[†] Academia Sinica.
[‡] Industrial Technology Research Institute.

(1) (a) Sheats, J. R.; Antoniadis, H.; Hueschen, M.; Leonard, W.; Miller, J.; Moon, R.; Roitman, D.; Stocking, A. *Science* **1996**, *273*, 884. (b) Ziemelis, K. *Nature* **1999**, *399*, 408. (c) Bradley, D. *Chem. Br.* **1999**, *August*, 22. (c) Dixon, R. *Compound Semiconductor* **1999**, *5* (Nov/Dec), 43. (d) Stinson, S. C. *Chem. Eng. News* **2000**, *June 26*, 22.

(2) Tang, C. W.; Van Slyke, S. A. *Appl. Phys. Lett.* **1987**, *51*, 913.

(3) (a) Burroughes, J. J.; Bradley, D. D. C.; Brown, A. R.; Marks, R. N.; Mackay, K.; Friend, R. H.; Burn, P. L.; Holmes, A. B. *Nature* **1990**, *347*, 539. (b) Friend, R. H.; Gymer, R. W.; Holmes, A. B.; Burroughes, J. H.; Marks, R. N.; Taliani, C.; Bradley, D. D. C.; Dos Santos, D. A.; Brédas, J. L.; Logdlund, M.; Salaneck, W. R. *Nature* **1999**, *397*, 121.

(4) (a) Gustafsson, G.; Cao, Y.; Treacy, G. M.; Klavetter, F.; Colaneri, N.; Heeger, A. J. *Nature* **1992**, *357*, 477. (b) Clery, D. *Science* **1994**, *263*, 1701. (c) Yam, P. *Sci. Am.* **1995**, *July*, 82.

(5) Justel, T.; Nikol, H.; Ronda, C. *Angew. Chem., Int. Ed. Engl.* **1998**, *37*, 3084.

10.1021/cm0008056 CCC: $20.00
Published on Web 08/17/2001

Amorphous thin films with high glass transition temperatures in OLEDs are less vulnerable to the joule heating, which accelerates the formation of crystalline boundaries. Bulky substituents and starburst molecular architecture are often adopted to enhance the solubility of molecules by preventing the molecules from stacking, which in turn favors the formation of amorphous glass materials. This molecular design strategy has been successfully applied to triarylamine-based hole-transporting materials.[7] 9,9-Dialkyl-substituted polyfluorenes, which exhibit reduced aggregation of polymer chains because of the sterically demanding sp^3-hybridized carbon, recently have become a new type of highly efficient polymer other than phenylenevinylene-based polymers for electroluminescence (EL).[8]

We and others recently have demonstrated that a rigid tetrahedral molecular skeleton, namely tetraphenylmethane, is effective for a stable amorphous phase of either molecular or oligomeric materials.[9] While EL properties of structure-related spiro compounds have been studied in detail,[10] corresponding properties of tetraphenylmethane-based compounds are still unknown. In the present work we will report the synthesis and thermal and EL properties of a series of tetraphenylmethane-based compounds. It is demonstrated that tetraphenylmethane is a useful structural unit for forming glassy films and is readily incorporated into light-emitting or charge-transporting materials by varying the peripheral substituents.

Experimental Section

General. ^{1}H and ^{13}C NMR spectra were recorded on a Brucker AMX-400 MHz or AC-300 MHz Fourier transform spectrometer at room temperature. Elemental analyses (on a Perkin-Elmer 2400 CHN elemental analyzer) and fast atom bombardment (FAB) mass spectra (on a VG Analytical 11-250J) were recorded by the Elemental Analyses and Mass Spectroscopic Laboratory in-house service of the Institute of Chemistry, Academia Sinica. UV−visible electronic absorption spectra were recorded on a Hewlett-Packard 8453 diode array spectrophotometer. Photoluminescence (PL) spectra were recorded on a Hitachi fluorescence spectrophotometer F-4500. Fluorescence quantum yields (Φ_f) of interesting compounds were determined relative to that of 2-phenyl-5-(4-biphenyl)-1,3,4-oxadiazole in benzene at 298 K ($\Phi_f = 0.8$).[11] Melting points (T_m), glass transition temperatures (T_g), and crystallization temperatures (T_c) of respective compounds were measured by differential scanning calorimetry (DSC) under nitrogen atmosphere using a Perkin-Elmer DSC-7 differential scanning calorimeter. Thermogravimetric analysis (TGA) was carried out on a Perkin-Elmer DSC-7 thermogravimetric analyzer to determine the decomposition temperatures (T_d) of the compounds under nitrogen atmosphere. Both thermal analyses were performed with a scanning (both heating and cooling) rate of 10 deg/min. We took the temperatures at the intercept of the slope of thermogram changes (endothermic, exothermic, or weight loss) and the leading baseline as the estimation for onset T_m, T_g, T_c, and T_d. Redox potentials of the compounds were determined by cyclic voltammetry (CV) using an Electochemical Analyzer BAS 100B with a scanning rate of either 100 or 1000 mV/s. The compound of interest was dissolved in deoxygenated dry DMF with 0.1 M tetrabutylammonium perchlorate as the electrolyte. We used a platinum working electrode and a saturated $Ag/AgNO_3$ referenced electrode. Ferrocene was used for potential calibration (all reported potentials are referenced against ferrocene/ferrocenium, FOC) and for reversibility criteria.

Materials. 2-(4-Biphenylyl)-5-(4-*tert*-butylphenyl)-1,3,4-oxadiazole (PBD), 2-(4-Biphenylyl)-5-phenyl-1,3,4-oxadiazole, tris(dibenzylidineacetone)dipalladium ($Pd_2(dba)_3$), diphenylphosphinoferrocene (dppf), and polyvinylcabazole (PVK) were obtained from Aldrich and used as received. Both tris(8-hydroxyquinoline)aluminum (Alq_3) and 1,4-bis(1-naphthylphenylamino)biphenyl (NPB) were also purchased from Aldrich but used after purification by sublimation. Several key compounds, such as tetrakis(4-cyanophenyl)methane and tetraphenylmethane-4,4′,4″,4‴-tetracarboxylic acid, and 4-tetraazolyltriphenylamine were known and synthesized according to the literature procedure.[12] Tetrakis(4-chlorocarbonylphenyl)methane was prepared by treating tetraphenylmethane-4,4′,4″,4‴-tetracarboxylic acid with an excess amount of thionyl chloride. Unreacted thionyl chloride was first removed with a rotatory evaporator. Any volatile liquid remained was then evaporated in vacuo at 50−70 °C. The obtained acid chlorides were used for subsequent reactions without further purification.

Tetrakis(4-tetraazolylphenyl)methane. Tetrakis(4-cyanophenyl)methane (5.00 g, 11.90 mmol) was added to a dried DMF solution (25 mL) containing NaN_3 (4.65 g, 71.35 mmol) and ammonium chloride (3.82 g, 71.35 mmol). The mixture was slowly heated to 100 °C for 24 h under nitrogen. Excess salts remained as a suspension even at high temperature. After the reaction mixture cooled, it was then acidified with 2 N HCl solution (*attention: hydrazoic acid is formed!*) until acidic conditions were reached, after which a white powder slowly appeared. The product was isolated by filtration and washed thoroughly with water to eliminate excess salts (*note: rapid absorption of moisture!*). The product was dried under reduced pressure in the presence of P_2O_5. Yield: 96% (6.85 g). ^{1}H NMR (300 MHz, d_6-DMSO): δ [ppm] 7.54 (d, 8H, $J = 8.5$ Hz), 8.02 (d, 8H, $J = 8.5$ Hz). $^{13}C\{^1H\}$ NMR (75 MHz, d_6-DMSO): δ [ppm] 155.0, 148.3, 131.2, 127.0, 122.4, 64.9. FAB-MS: calcd MW, 592.21, $m/e = 592$ (M^+). Anal. Found (calcd) for $C_{29}H_{20}N_{16}\cdot 2H_2O$: C, 55.41 (55.44); H, 3.80 (3.85); N, 35.31 (35.68).

Tetrakis(4-(5-(3,4-dimethoxyphenyl)-2-oxadiazolyl)-phenyl)methane (OMEOXD). Tetrakis(4-tetraazolylphenyl)-methane (1.18 g, 2.0 mmol) was dissolved in dried anisole (50 mL) containing 3,4-dimethoxybenzoyl chloride (1.76 g, 8.8 mmol). 2,4,6-Collidine (1.2 mL) was added dropwise to the mixture with stirring. After the addition of collidine, the

(6) (a) Service, R. F. *Science* **1996**, *273*, 878. (b) Conwell, E. *Trends Polym. Sci.* **1997**, *5*, 218.

(7) (a) O'Brien, D. F.; Burrows, P. E.; Forrest, S. R.; Konne, B. E.; Loy, D. E.; Thompson, M. E. *Adv. Mater.* **1998,** *10*, 1108. (b) Konne, B. E.; Loy, D. E.; Thompson, M. E. *Chem. Mater.* **1998**, *10*, 2235. (c) Shirota, Y. *J. Mater. Chem.* **2000**, *10*, 1 and refeences therein.

(8) (a) Fukada, M.; Sawaka, K.; Yoshino, K. *Jpn. Appl. Phys., Part 2* **1989**, *28*, L1433. (b) Pei, Q.; Yang, Y. *J. Am. Chem. Soc.* **1996**, *118*, 7416. (c) Griece, A. W.; Bradley, D. D. C.; Bernius, M. T.; Inbasekaran, M.; Wu, W. W.; Woo, E. P. *Appl. Phys. Lett.* **1998**, *73*, 629. (d) Yu, W.-L.; Pei, J.; Huang, W.; Heeger, A. J. *Adv. Mater.* **2000**, *12*, 828.

(9) (a) Oldham, W. J., Jr.; Lachicotte, R. J.; Bazan, G. C. *J. Am. Chem. Soc.* **1998**, *120*, 2987. (b) Wang, S.; Oldham, W. J., Jr.; Hudack, R. A.; Bazan, G. C. *J. Am. Chem. Soc.* **2000**, *122*, 5695. (c) Chen, C.-T.; Lin, T.-Y. J.; Jan, L.-H.; Yeh, H.-C.; Balasubramaniam, E.; Tao, Y.-T. *Mater. Res. Soc. Proc.* **2000**, *598*, BB3.5.1. (d) Yeh, H.-C.; Chan, L.-H.; Lee, R.-H.; Chen, C.-T. *SPIE−Int. Soc. Opt. Eng.* **2000**, *4105*, 348.

(10) (a) Salbeck, J.; Yu, N.; Bauer, J.; Weissörtel, F.; Bestgen, H. *Synth. Met.* **1997**, *91*, 209. (b) Salbeck, J.; Bauer, J.; Weissörtel, F. *Macromol. Symp.* **1997**, *125*, 121. (c) Johansson, N.; dos Santos, D. A.; Guo, S.; Cornil, J.; Fahlman, M.; Salbeck, J.; Schenk, H.; Arwin, H.; Brédas, J. L.; Salenek, W. R. *J. Chem. Phys.* **1997**, *107*, 2542. (d) Weinfurtner, K.-H.; Weissörtel, F.; Harmgarth, G.; Salbeck, J. *SPIE−Int. Soc. Opt. Eng.* **1998**, *3476*, 40. (e) Lupo, D.; Salbeck, J.; Schenk, H.; Stehlin, T.; Stern, R.; Wolf, A. U.S. Patent No. 5840217, 1998. (e) Kreuder, W.; Lupo, D.; Salbeck, J.; Schenk, H.; Stechlin, T. U.S. Patent No. 5859211, 1999. (f) Steuber, F.; Staudigel, J.; Stössel, M.; Simmerer, J.; Winnacker, A.; Spreitzer, H.; Weissörtel, F.; Salbeck, J. *Adv. Mater.* **2000**, *12*, 130.

(11) (a) Demas, J. N.; Crosby, G. A. *J. Phys. Chem.* **1971**, *75*, 991. (b) Fouassier, J.-P.; Lougnot, D.-J.; Wieder, F.; Faure, J. *J. Photochem.* **1977**, *7*, 17.

(12) (a) Grimm, M.; Kieste, B.; Kurreck, H. *Angew. Chem., Int. Ed. Engl.* **1986**, *24*, 1097. (b) Tamoto, N.; Adachi, C.; Nagai, K. *Chem. Mater.* **1997**, *9*, 1077.

solution was stirred for 3 h at ~110 °C under nitrogen atmosphere. During the stirring, a white precipitate gradually emerged. The solution was subjected to flash column chromatography (silica gel, chloroform with 10% ethyl acetate as eluent). The first bright purplish blue band (under long-wavelength UV light) developed was collected. Yield: 50% (1.09 g). ^{1}H NMR (400 MHz, $CDCl_3$): δ [ppm] 8.10 (d, 8H, J = 8.3 Hz), 7.65 (dd, 4H, J = 8.4, 2.0 Hz), 7.64 (d, 4H, J = 2.0 Hz), 7.47 (d, 8H, J = 8.3 Hz), 6.97 (d, 4H, J = 8.4 Hz), 3.97 (s, 12H), 3.94 (s, 12H). ^{13}C{^{1}H} NMR (100 MHz, $CDCl_3$): δ [ppm] 164.6, 163.6, 152.1, 149.4, 148.5, 131.3, 126.7, 122.6, 120.4, 116.3, 111.1, 109.4, 65.5, 56.1, 56.0. FAB-MS: calcd MW, 1136.37, m/e = 1136 (M^+). Anal. Found (calcd) for $C_{65}H_{58}N_8O_{15}$ (OMEOXD·3H_2O): C, 66.17 (65.53); H, 4.88 (4.91); N, 8.25 (9.41).

Tetrakis(4-(5-(3,5-di-*tert*-butylphenyl)-2-oxadiazolyl)-phenyl)methane (TBUOXD). Tetrakis(4-tetraazolylphenyl)-methane (0.89 g, 1.5 mmol) was reacted with 3,5-di-*tert*-butylbenzoyl choloride (1.70 g, 6.6 mmol) in a similar manner as in the synthesis of OMEOXD. The first bright blue band (under long-wavelength UV light) developed during flash column chromatography (silica gel, dichloromethane with 5% ethyl acetate as eluent) was collected. Yield: 70% (1.40 g). ^{1}H NMR (400 MHz, $CDCl_3$): δ [ppm] 8.14 (d, 8H, J = 8.6 Hz), 7.94 (d, 8H, J = 1.5 Hz), 7.60 (t, 4H, J = 1.5 Hz), 7.50 (d, 8H, J = 8.6 Hz), 1.37 (s, 72H). ^{13}C{^{1}H} NMR (100 MHz, $CDCl_3$): δ [ppm] 165.5, 163.8, 151.9, 148.6, 131.4, 126.9, 126.1, 123.1, 122.7, 121.2, 66.5, 35.0, 31.3. FAB-MS: calcd MW, 1344.79, m/e = 1344 (M^+). Anal. Found (calcd) for $C_{29}H_{24}N_{16}O_2$ (TBUOXD·2H_2O): C, 77.13 (77.36); H, 7.35 (7.59); N, 7.85 (8.11).

Tetrakis(4-(5-(3-(α,α,α-trifluoromethylphenyl))-2-oxadiazolyl)phenyl)methane (CF3OXD). Tetrakis(4-tetraazolylphenyl)methane (2.69 g, 5.0 mmol) was reacted with 3-(trifluoromethyl)benzoyl choloride (3.3 mL, 22.0 mmol) in a similar manner as in the synthesis of OMEOXD. The first bright blue band (under long-wavelength UV light) developed during flash column chromatography (silica gel, dichloromethane with 15% ethyl acetate as eluent) was collected. Yield: 92% (5.40 g). ^{1}H NMR (400 MHz, $CDCl_3$): δ [ppm] 8.35 (s, 4H), 8.33 (d, 4H, J = 8.2 Hz), 8.15 (d, 8H, J = 8.4 Hz), 7.89 (d, 4H, J = 8.2 Hz), 7.68 (t, 4H, J = 8.2 Hz), 7.51 (d, 8H, J = 8.4 Hz),. ^{13}C{^{1}H} NMR (100 MHz, $CDCl_3$): δ [ppm] 164.4, 163.5, 148.8, 131.8 (q, J_{CF} = 33 Hz), 131.4, 130.0, 129.8, 128.3, 127.0, 124.6, 123.7, 123.4 (q, J_{CF} = 271 Hz), 122.2, 65.6. FAB-MS: calcd MW, 1168.24, m/e = 1169 ($M + 1^+$). Anal. Found (calcd) for $C_{61}H_{32}F_{12}N_8O_4$ (CF3OXD): C, 62.01 (62.68.44); H, 2.67 (2.76); N, 9.10 (9.59).

Tetrakis(4-(5-(4-diphenylaminophenyl)-2-oxadiazolyl)-phenyl)methane (*p*-TPAOXD). Tetrakis(4-chlorocarbonylphenyl)methane (0.57 g, 1.0 mmol) was reacted with 4-tetraazoyltriphenylamine (1.5 g, 4.8 mmol) in a similar manner as in the synthesis of OMEOXD. The second bright green band (under long-wavelength UV light) developed during flash column chromatography (silica gel, 19 part dichloromethane vs 1 part ethyl acetate) was collected. Yield: 50% (0.78 g).^{1}H NMR (400 MHz, $CDCl_3$): δ [ppm] 8.06 (d, 8H, J = 8.7 Hz), 7.90 (d, 8H, J = 8.9 Hz), 7.45 (d, 8H, J = 8.65 Hz), 7.27−7.33 (m, 16H), 7.14 (d, 16H, J = 8.5 Hz), 7.06−7.12 (m, 16H). ^{13}C-{^{1}H} NMR (100 MHz, $CDCl_3$): δ [ppm] 164.6, 163.3, 151.0, 148.4, 146.5, 131.3, 129.5, 127.9, 126.6, 125.6, 124.4, 122.6, 120.9, 115.7, 65.4. FAB-MS: calcd MW, 1564.58, m/e = 1566 ($M + 1^+$). Anal. Found (calcd) for $C_{105}H_{72}N_{12}O_4$ (*p*-TPAOXD): C, 80.40 (80.54); H, 4.80 (4.63); N, 10.63 (10.73).

3-Cyanotriphenylamine. To a solution of $Pd_2(dba)_3$ (0.21 g, 0.22 mmol) and dppf (0.19 g, 0.33 mmol) in dry toluene (30 mL) under nitrogen atmosphere was added 3-bromobenzonitrile (4.04 g, 22.0 mmol) at room temperature, and the resultant mixture was stirred for 10 min. Then, potassium *tert*-butoxide (2.81 g, 25.0 mmol) and diphenylamine (3.39 g, 20.0 mmol) were added. The solution was refluxed for 20 h. After it was cooled to room temperature, the mixture was worked up with the standard procedure and purified by flash column chromatography (silica gel, hexanes with 10% dichloromethane as eluent). Yield: 50% (2.98 g). ^{1}H NMR (400 MHz, $CDCl_3$): δ [ppm] 7.26−7.33 (m, 4H), 7.21−7.25 (m, 3H), 7.15 (ddd, 1H, J = 7.0, 2.4, 0.8 Hz), 7.05−7.13 (m, 6H). ^{13}C{^{1}H} NMR (100 MHz, $CDCl_3$): δ [ppm] 148.1, 146.0, 129.5, 129.2, 125.5, 124.6, 124.2, 124.1, 123.8, 118.1, 112.6.

3-Tetraazolyltriphenylamine. This compound was synthesized according to the literature procedure for preparing 4-tetraazolyltriphenylamine.[11b] Yield: 50%. ^{1}H NMR (400 MHz, d_6-DMSO): δ [ppm] 7.66 (t, 1H, J = 1.8 Hz), 7.63 (d, 1H, J = 7.8 Hz), 7.47 (t, 1H, J = 7.8 Hz), 7.34 (t, 4H, J = 7.6 Hz), 7.04−7.13 (m, 7H). ^{13}C{^{1}H} NMR (100 MHz, d_6-DMSO): δ [ppm] 155.3, 148.5, 147.0, 130.8, 130.0, 125.5, 125.3, 124.7, 124.0, 120.7.

Tetrakis(4-(5-(3-diphenylaminophenyl)-2-oxadiazolyl)-phenyl)methane (*m*-TPAOXD). Tetrakis(4-chlorocarbonylphenyl)methane (0.57 g, 1.0 mmol)was reacted with 4-tetraazolyltriphenylamine (1.4 g, 4.5 mmol) in a similar manner as in the synthesis of OMEOXD. The second bright green band (under long-wavelength UV light) developed during flash column chromatography (silica gel, 19 part dichloromethane vs 1 part ethyl acetate) was collected. Yield: 60% (0.93 g). ^{1}H NMR (400 MHz, $CDCl_3$): δ [ppm] 8.02 (d, 8H, J = 8.7 Hz), 7.79 (t, 4H, J = 1.9 Hz), 7.69 (dt, 4H, J = 7.7, 1.3 Hz), 7.41 (d, 8H, J = 8.7 Hz), 7.35 (t, 4H, J = 7.9 Hz), 7.24−7.30 (m, 16H), 7.21 (ddd, 4H, J = 8.2, 2.3, 0.9 Hz), 7.07−7.13 (m, 16H), 7.05 (t, 8H, J = 7.3 Hz). ^{13}C{^{1}H} NMR (100 MHz, $CDCl_3$): δ [ppm] 164.6, 163.9, 148.8, 148.6, 147.2, 131.3, 130.0, 129.5, 126.8, 126.5, 124.8, 124.6, 123.6, 122.4, 121.1, 120.5, 65.5. FAB-MS: calcd MW, 1564.58, m/e = 1566 ($M + 1^+$). Anal. Found (calcd) for $C_{105}H_{72}N_{12}O_4$ (*m*-TPAOXD): C, 80.38 (80.54); H, 4.74 (4.63); N, 10.73 (10.73).

Fabrication and Characterization of Light-Emitting Devices. *Multilayer Devices.* OLED devices containing CF3OXD were fabricated by vacuum-deposition. The substrate was an indium tin oxide (ITO)-coated glass with a sheet resistance of <50 Ω/sq. The pretreatment of ITO includes a routine chemical cleaning using detergent and alcohol in sequence, followed by oxygen plasma cleaning. The thermal evaporation of organic materials was carried out using ULVAC Cryogenics at a chamber pressure of 10^{-6} Torr. The cathode $Mg_{0.9}Ag_{0.1}$ alloy was deposited (50 nm) by coevaporation and followed by a thick silver capping layer. The effective size of the emitting diode was 3.14 mm^2. Current−voltage−luminescence (I−V−L) measurements were made simultaneously using a Keithley 2400 Source meter and a Newport 1835C optical meter equipped with a Newport 818-ST silicon photodiode, respectively. The measurements were made at room temperature under ambient conditions. The EL was measured using the fluorescence spectrophotometer by blocking the incident light.

Single-Layer Devices. Amorphous thin films of *p*-TPAOXD, *m*-TPAOXD, or a blending of *p*-TPAOX**D** and PVK (~1000 or 1200 Å) were formed by spin-casting from tetrahydofuran or cyclohexanone solution (15 or 25 mg/mL) onto indium tin oxide (ITO)-coated glass (with a resistance of 15 Ω/sq) substrates. The thickness of the film was determined with a surface texture analysis system (Dektak 3030ST). A high-purity calcium cathode (150 Å) was thermally deposited at right angles on the *p*-TPAOXD thin film followed by the deposition of silver metal (2500 Å) as the top layer. A LiF thin film (10 Å) was thermally deposited followed by the deposition of aluminum metal (2500 Å) as the top layer. The active emitting area was controlled to be 1 × 1 cm^2. EL spectra of the OLED devices were measured with the fluorescence spectrophotometer (Hitachi F4500). The current−voltage characteristics were measured on a programmable electrometer having current and voltage sources (Keithley). The luminance was measured with a luminance meter BM-8 (TOPCON).

Results and Discussion

Synthesis. The tetraphenylmethane-based 1,3,4-oxadiazole compounds TBUOXD, OMEOXD, and CF3OXD were all prepared similarly with good yields (50−92%) by reacting tetrazole derivative with benzoyl chloride carrying the appropriate substituents (Scheme 1) in a

Scheme 1

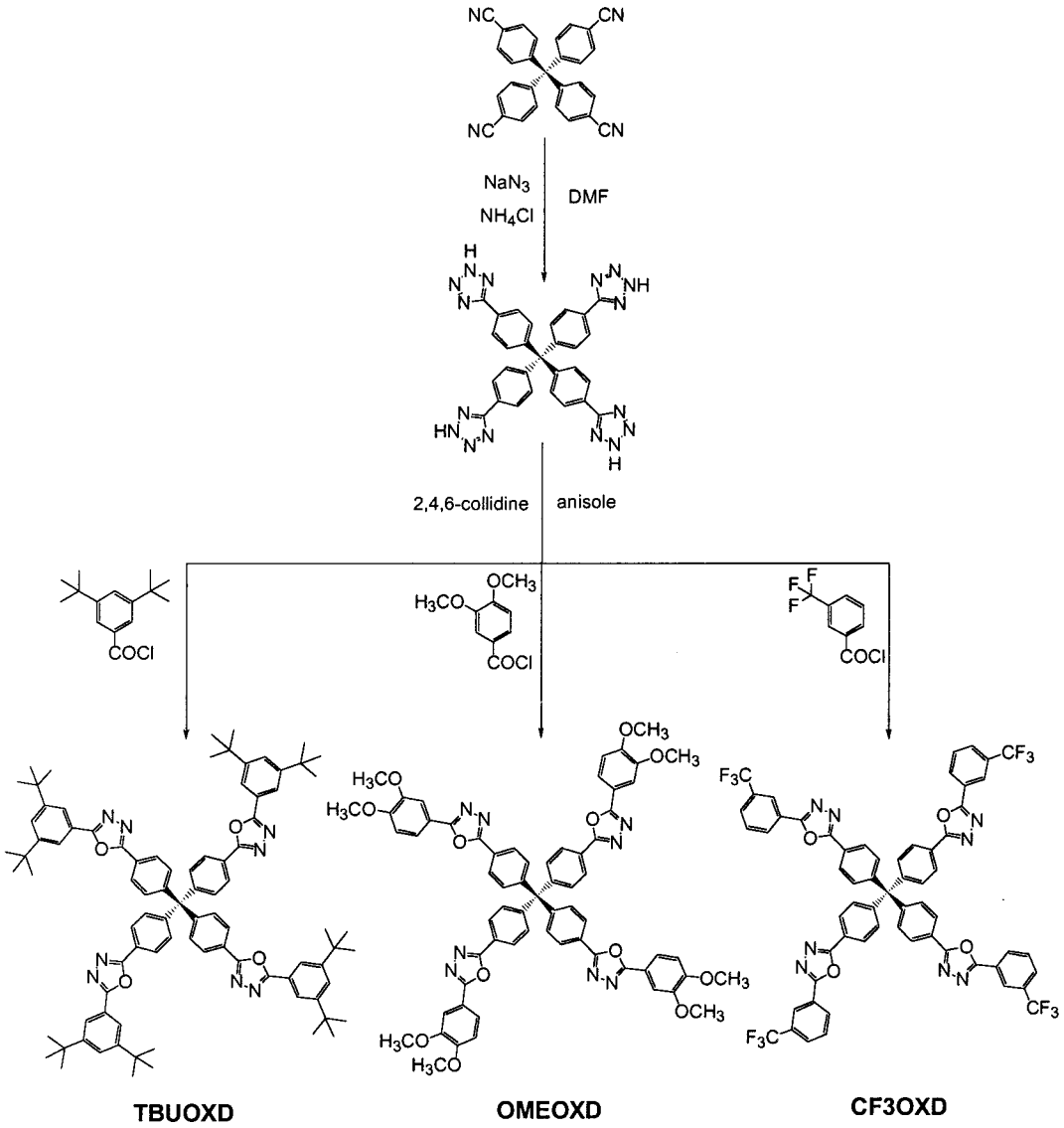

modified Huisgen reaction.[13] We chose commercially available 3,4-dimethoxybenzoyl chloride and 3-(trifluoromethyl)benzoyl chloride as well as readily synthesized 3,5-di-*tert*-butylbenzoyl chloride[14] for an illustrative purpose. The previously unknown tetrakis(4-tetraazolylphenyl)methane was synthesized in quantitative yield by the reaction of sodium azide and ammonium chloride with known 4,4′,4″,4‴-tetracyanotetraphenylmethane.[15] All new compounds were fully characterized by elemental analysis, FAB-MS, and ^{1}H and ^{13}C NMR spectroscopies.

A similar approach, that is, the reaction of tetrakis(4-tetraazolylphenyl)methane with substituted benzoyl chloride, in synthesizing the bipolar tetramers *m*-TPAOXD and *p*-TPAOXD was unsuccessful due to the failure in preparing diphenylamino-bearing benzoyl chloride. An alternative route was adopted, in which the acid chloride groups were attached to tetraphenylmethane and the tetraazole rings were connected to triphenylamine, as shown in Scheme 2. Both *m*-TPAOXD and *p*-TPAOXD were prepared with reasonably good yields (>60%). While *p*-tetraazolyltriphenylamine was a known compound, previously unknown *m*-tetraazolyltriphenylamine was synthesized in two-step reactions, first by Pd-catalyzed coupling of *m*-bromobenzonitrile with diphenylamine. *m*-Tetraazolyltriphenylamine was obtained after the reaction of *m*-cyanotriphenylamine with sodium azide and ammonium chloride in dry DMF by a method similar to that used in preparing *p*-tetraazolyltriphenylamine.

Characterization of TBUOXD, OMEOXD, and CF3OXD. These three compounds are either white or off-white solids with the absorption maximum (λ_{max}^{ab}) occurring in the narrow range 292−315 nm in solution (Table 1). Among these oxadiazole compounds, the smallest shift (blue-shifted by 7 nm) of λ_{max}^{em} relative to that of PDB was found for TBUOXD, which has a *tert*-butyl substituent on the meta position that hardly affects the electronic state of the oxadiazole ring. These spectroscopic observations also indicate that the tetrameric tetrahedral framework has little or no effect on

(13) Detert, H.; Schollmeier, D. *Synthesis* **1999**, 999.
(14) Van Hartingsveldt, W.; Verkade, P. E.; Wepster, B. M. *Recl. Trav. Chim. Pay-Bas* **1956**, *75*, 349.
(15) (a) Bettenhausen, J.; Strohriegl, P. *Adv. Mater.* **1996**, *8*, 507. (b) Kieste, B.; Grimm, M.; Kurreck, H. *J. Am. Chem. Soc.* **1989**, *111*, 108.

Scheme 2

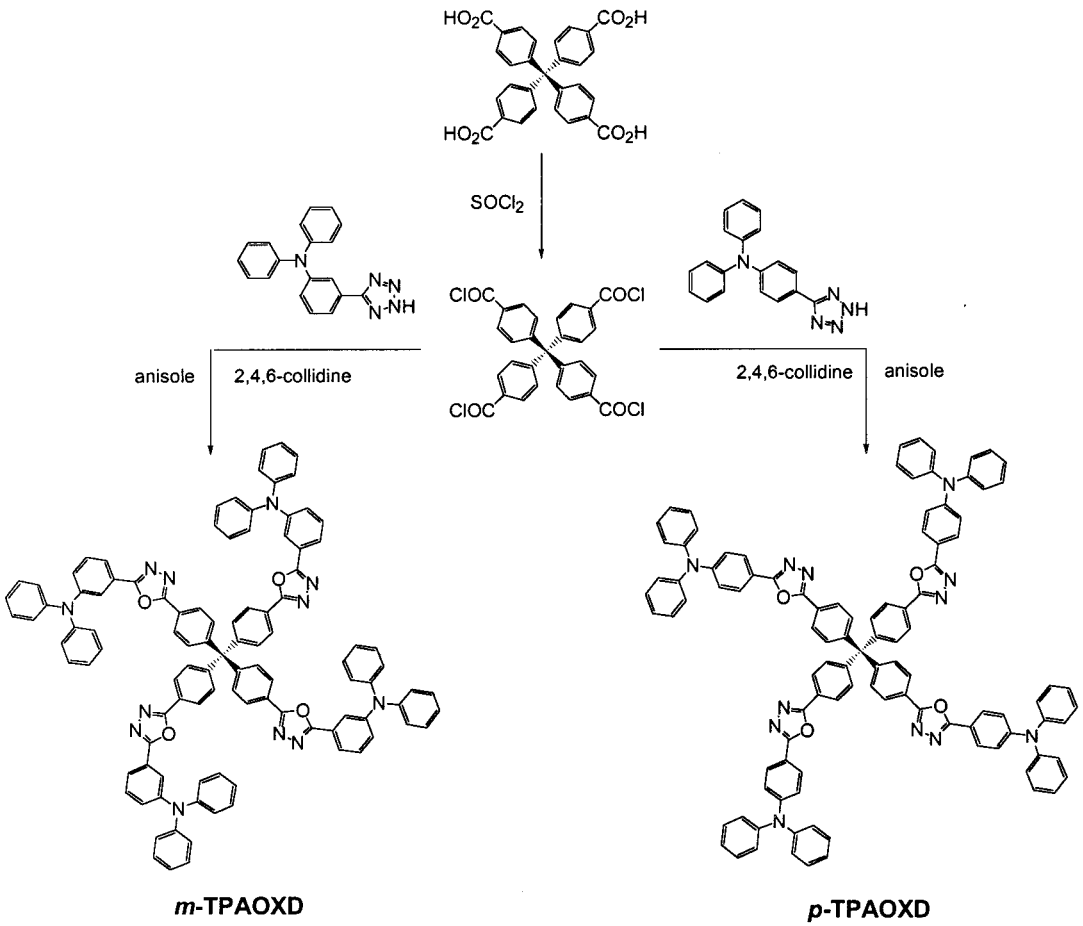

Table 1. Absorptive, Fluorescent, Thermal, and Redox Properties of TBUOXD, OMEOXD, CF3OXD, and PBD

compound	λ_{max}^{ab} (nm)[a]	λ_{max}^{em} (nm)[a]	ϕ_f[c]	T_g (°C)	T_c (°C)	T_m (°C)	T_d (°C)	E^{red} (eV) vs FOC
TBUOXD	296	372	0.8	175	205	400	405	−2.40 to −2.45
OMEOXD	315	386	0.9	97	227	337	428	∼−2.50
CF3OXD	292	370	0.8	125	202	270	499	−2.30
PBD	303	361	0.8	*b*	70−90	137	308	−2.42

[a] Measured in ethyl acetate solution. [b] Not observed. [c] In benzene.

the π-conjugation system of the oxadiazole moiety. The spectroscopic findings here differ somewhat from those reported for the tetrakis(styrylstilbenyl)methane derivative,[9a] in which case the π-systems of the four styrylstilbene units seem to interact with each other, despite a nonplanar sp^3-hybridized carbon in between. These compounds fluoresce purplish blue (TBUOXD and CF3OXD) to blue (OMEOXD) both in solution and in the solid state. The solution fluorescence quantum efficiencies (ϕ_f's) of TBUOXD, OMEOXD, CF3OXD, and PBD, a molecular material often used as an electron-transporting material in OLEDs, were determined (Table 1), and they were all comparable, with $\phi_f = 0.8-0.9$. Although there are no consistent shifts in λ_{max}^{ab} relative to that of PBD, the three oxadiazole derivatives all have fluorescence maximums (λ_{max}^{em}) about 10−25 nm red-shifted relative to that of PBD (Table 1). Such red-shifted spectra are, however, in accord with those of tetrakis(styrylstilbenyl)methane derivatives and styrylstilbene.[9a]

CV measurements showed that the compounds TBUOXD, OMEOXD, and CF3OXD as well as PBD have rather similar voltammogram features with comparable potentials of the first reduction process (Table 1). Like PBD, TBUOXD, OMEOXD, and CF3OXD did not show reversible reduction voltammograms indicating all of these oxadiazole-containing species have unstable reduced forms under electrochemical conditions. CV data also imply that the teraphenylmethane framework or peripheral substituents hardly alter the electron-capture tendency of the oxadiazole ring in the three oxadiazole derivatives compared with that of PBD.

Although similar in spectroscopic and electrochemical behavior, TBUOXD, OMEOXD, and CF3OXD are very different in thermal properties in comparison with PBD. In DSC measurements, a distinct endothermic peak at 137 °C, corresponding to the melting temperature of PBD, was observed. The crystallization temperature (T_c) of PBD was detected during the cooling cycle and varied between 70 and 90 °C. The melting points (T_m's) of TBUOXD, OMEOXD, and CF3OXD were determined to be ∼410, 320, and 260 °C, respectively, all higher than that of PBD. Exothermic onset T_c's around 200, 220, and 210 °C were also observed for TBUOXD, OMEOXD, and CF3OXD, respectively. Onset decomposition temperatures (T_d's) determined by TGA varied

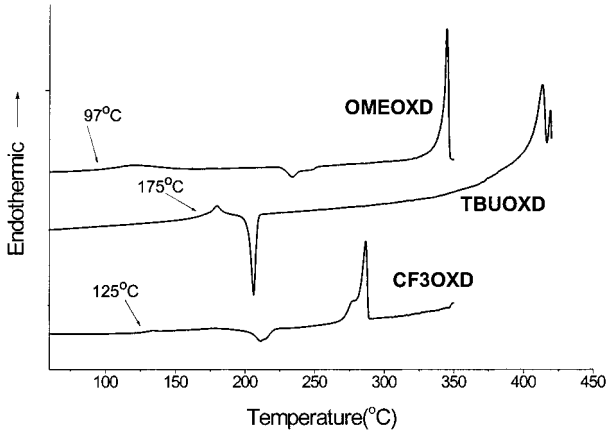

Figure 1. DSC scans of TBUOXD, OMEOXD, and CF3OXD. Onset T_g's were marked on each thermogram.

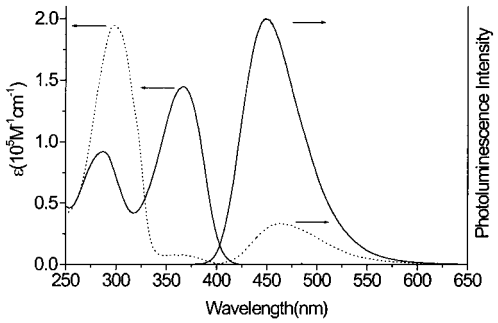

Figure 2. Absorption spectra and fluorescence spectra of *m*-TPAOXD (dotted lines) and *p*-TPAOXD (solid lines). The relative intensity of fluorescence spectra is scaled on the basis of the fluorescence quantum efficiency of *m*-TPAOXD and *p*-TPAOXD.

between 400 and 500 °C depending on the peripheral substituent of the compounds (Table 1). These T_d's are all significantly higher than that of PBD (T_d = 308 °C). In addition, careful examination of DSC thermograms revealed that endothermic step transitions persistently appeared at ~175, 97, and 125 °C, which were assigned to the onset glass transition temperatures of the three oxadiazole compounds (Figure 1). In contrast, no possible glass transition signal was detected for PBD in repeated heating−cooling DSC cycles. Thus, the tetraphenylmethane structural approach is effective at raising T_m, T_c, and T_d, and more importantly inducing T_g of oxadiazole compounds.

Characterization of *m*-TPAOXD and *p*-TPAOXD. Because of the different substitution positions of the diphenylamino donor group on the 2,5-diphenyl-1,3,4-oxadiazole, there are some interesting features on the absorption and fluorescence spectra of *m*-TPAOXD and *p*-TPAOXD (Figure 2). *p*-TPAOXD has two major absorption bands at 287 and 366 nm, with extinction coefficients near and over 10^5, respectively. The absorption band pattern is very similar to that of the benzene ring-connected dimer and trimer of 4-(1,3,4-oxadiazol-2-yl)triphenylamine.[12b] In constrast, *m*-TPAOXD shows only one major absorption band at 298 nm, accompanied by a shoulder at ~320 nm as well as a weak and broad absorption band around 365 nm. The absorption band of *p*-TPAOXD with a maximum at 366 nm may be attributed to the charge-transfer absorption band due to the π-conjugation between triphenylamine and oxadiazole units, which is absent in meta-substituted

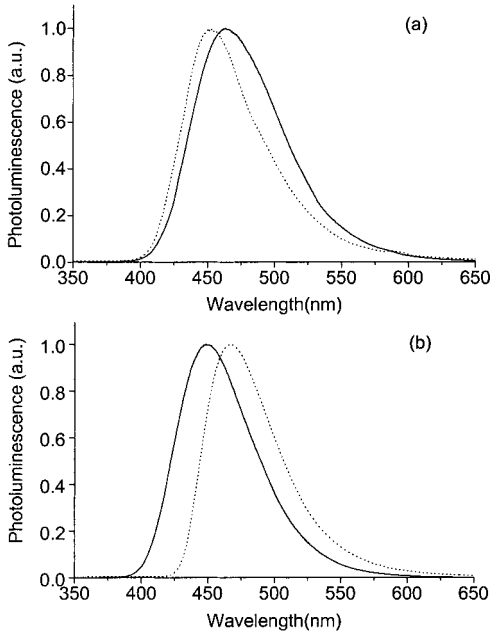

Figure 3. (a) Fluorescence spectra of *p*-TPAOXD in dichloromethane (solid line) and in the solid film state (dotted line). (b) Fluorescence spectra of *m*-TPAOXD in dichloromethane (solid line) and in the solid film state (dotted line).

m-TPAOXD. Therefore, it is not too surprising to find that the fluorescence intensity of *p*-TPAOXD (ϕ_f ~ 50%) is about six times stronger than that of *m*-TPAOXD (ϕ_f ~ 9%) because of the conjugated para-substitution of the π-excessive/π-deficient moiety in *p*-TPAOXD.

Figure 3 compares the PL spectra of both *m*-TPAOXD and *p*-TPAOXD in solution and as solid films. The differences of the emission maximum under the two conditions are relatively small for both compounds. There is a 19 nm red-shift and a 8 nm blue-shift from solution to solid film of *p*-TPAOXD and *m*-TPAOXD, respectively. The opposite shifting-directions of the PL spectrum found for *m*-TPAOXD and *p*-TPAOXD may be due to the different electronic structures of the two compounds. *p*-TPAOXD shows more charge-transfer characteristics than *m*-TPAOXD, as indicated by their quite different absorption spectra. In addition, both compounds have rather similar emission bandwidths in solution and in the solid film state. The above-mentioned spectroscopic characteristics are indicative of little excimer formation in the solid state, which in turn implies a homogeneous amorphous film with limited intermolecular contact. It is noteworthy that *m*-TPAOXD has a significantly smaller difference between solution and solid film emission spectra. This can be attributed to *m*-TPAOXD's bend-shaped dipolar diphenylaminophenyl-substituted oxadiazole moieties, which leave limited space for interchromophore contact through interpenetration. Similar phenomena were also known for stilbenoid-substituted tetraphenylmethanes.[9b]

The amorphous glass-forming nature of both *m*-TPAOXD and *p*-TPAOXD was fully revealed from DSC. Figure 4 shows the repeated DSC heating and cooling (10 °C/min) scan cycles of the sample of *p*-TPAOXD. It is evident that the sample shows only an endothermic steplike transition around 190 °C, which was assigned as T_g of *p*-TPAOXD (the onset T_g was estimated to be ~187 °C). No indication of T_c or T_m could be located from

Table 2. Optical, Electrochemical, and Thermal Properties of *m*-TPAOXD and *p*-TPAOXD

	λ_{max}^{ab} (log ϵ) (nm)[a]	λ_{max}^{em} solution (nm)[a]	λ_{max}^{em} solid film (nm)	ϕ_f	E^{ox} vs FOC (V)	E^{red} vs FOC (V)	T_g (°C)	T_d (°C)
m-TPAOXD	298 (5.29)	463	451	0.1	0.62	−2.31	149	464
p-TPAOXD	287 (4.96), 366 (5.16)	448	467	0.5	0.65	−2.37	187	474
NPB	270,[c] 340[c]	450[c]	*b*	*b*	0.30	*b*	100[c]	*b*

[a] In dichloromethane [b] Not measured [c] From ref 7b.

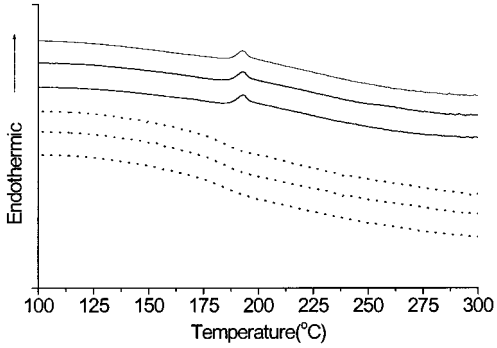

Figure 4. DSC scans of *p*-TPAOXD: from top to bottom, the second, third, and fourth heating scans (solid lines); the first, second, and third cooling scans (dotted lines).

all the thermograms (scan temperatures between 40 and 400 °C) of *p*-TPAOXD. A T_g is generally used as a stability indicator for the amorphous state in polymers. However, it is quite unusual that molecular materials do not possess a melting point (T_m) or crystallization temperature (T_c) but exhibit only T_g. The phase behavior of *p*-TPAOXD is in fact rather similar to that of a polymer sample with a high T_g. A similar DSC thermogram was observed for *m*-TPAOXD with the onset T_g located at ∼149 °C (Table 2). The presence of observed T_g's for both *m*-TPAOXD and *p*-TPAOXD may have the same bearing as the insensitivity of λ_{max}^{em} in solution and in the solid film state, that is, weak intermolecular contact and hence low tendency of crystallization. Thermally, both compounds are robust and their TGA-determined onset T_d's are 464 and 474 °C, respectively (Table 2).

The redox potentials of both *m*-TPAOXD and *p*-TPAOXD were determined by CV, and they were rather similar. The first oxidation process is reversible. However, the first reduction process is reversible at a fast scanning rate (1 V/s) and becomes irreversible at a low scanning rate (100 mV/s). Within the experimental error, which is about ±50 mV, both compounds have a rather similar first oxidation potential around 0.62−0.65 V versus FOC and the first reduction potential around −2.31 to −2.37 V versus FOC (Table 2). However, these numbers imply that both compounds have a significantly lower HOMO energy level relative to that of NPB (E^{ox} = 0.30 V versus FOC) and a slightly lower or comparable LUMO energy level than that of PBD (E^{red} = −2.42 V versus FOC). On the basis of CV redox data, both dipolar compounds are expected to behave more like an electron-transporting (or hole-blocking) material rather than a hole-transporting material in OLED applications. This conclusion is in general accord with what was found earlier for 1,4-bis(2-diphenylaminooxadiazol-5-yl)benzene.[12b] Nevertheless, the true charge-transporting nature of *m*-TPAOXD and *p*-TPAOXD will be identified by further charge-mobility studies.

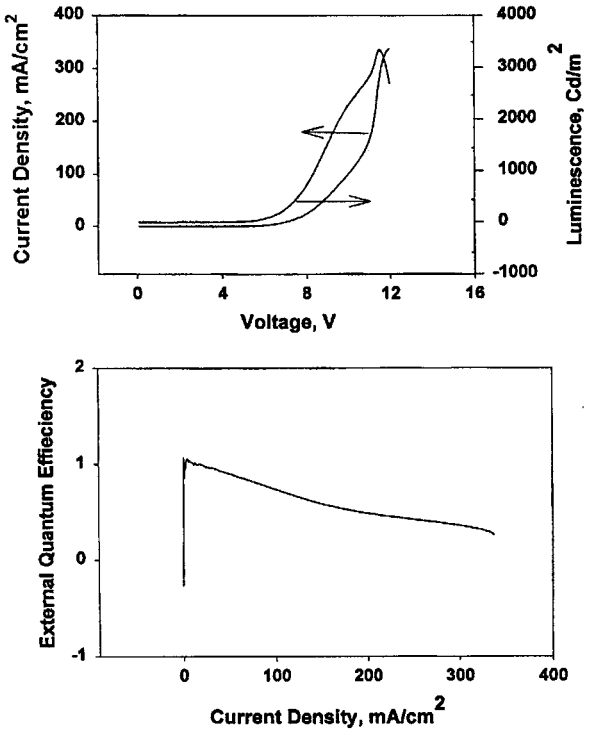

Figure 5. *I*−*V*−*L* characteristics of the device ITO/NPB/Alq_3/PBD/ Mg:Ag.

Characterization of Light-Emitting Devices Containing CF3OXD. A three-layer OLED device with a structure of ITO/NPB (400 Å)/Alq_3 (50 Å)/CF3OXD (400 Å)/Mg:Ag was constructed by vacuum deposition on the ITO-coated glass substrate. CF3OXD was chosen for device fabrication because of its acceptable volatility under high vacuum. A reference device of ITO/NPB (400 Å)/Alq_3 (50 Å)/PBD (400 Å)/Mg:Ag was also constructed for comparison. Both devices started glowing at 7−8 V applied bias voltage with green luminescence (λ_{max}^{em} ∼ 515 nm), a characteristic EL from Alq_3. Nevertheless, differences between the two OLED devices were notable in terms of *I*−*V*−*L* (Figures 5 and 6). First, the allowed current densities (mA/cm^2) in both devices were quite different. At a drive voltage of 12 V, the current was three times lower in the device containing CF3OXD than in that containing PBD, indicative of higher current resistance in the CF3OXD-based device. Furthermore, the CF3OXD-based device was more than three times dimmer than the PBD-based device under the same drive voltage (10 V). Therefore, with a smaller current density as well as weaker EL, the CF3OXD-based device still has a comparable maximum external quantum efficiency of ∼0.75% to ∼1% (both occur at a drive voltage around 8 V) of that of the PBD-based device.

Characterization of Light-Emitting Devices Containing *p*-TPAOXD or *m*-TPAOXD. We have also used strongly blue fluorescent *p*-TPAOXD to fabricate

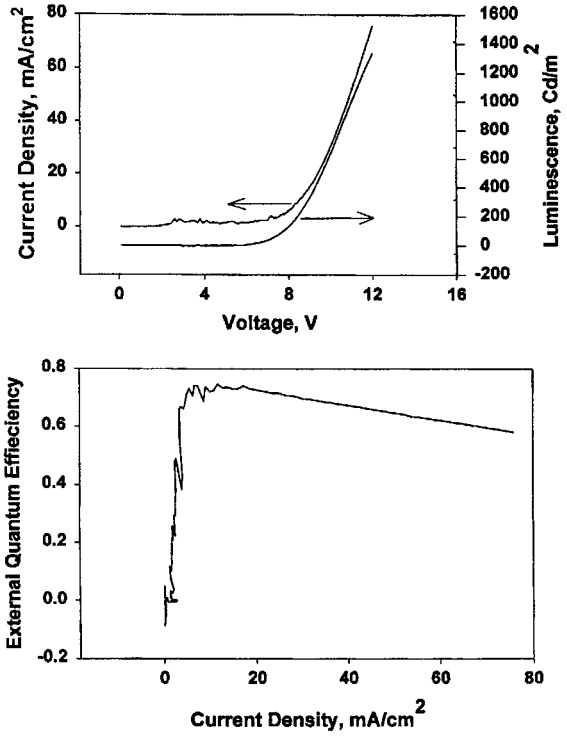

Figure 6. $I-V-L$ characteristics of the device ITO/NPB/Alq_3/CF3OXD/Mg:Ag.

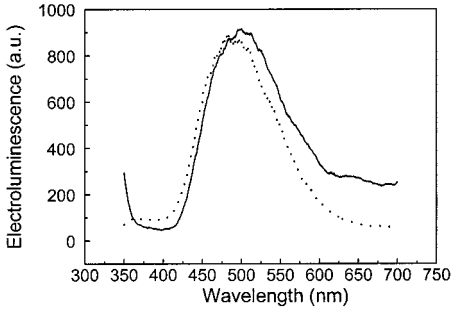

Figure 7. EL spectra of the devices ITO/*p*-TPAOXD (THF, 1000 Å)/Ca/Ag (solid line) and ITO/*p*-TPAOXD (THF, 1300 Å)/LiF/Al (dotted line).

single-layer devices. The EL, $I-V-L$, and power efficiency (lm/W) characteristics are shown in Figures 7 and 8. As can be seen in Figure 7, λ_{max}^{em} (~480−490 nm) of the EL spectrum of *p*-TPAOXD is about 20−30 nm red-shifted compared to that of the PL spectrum of the solid film (shown in Figure 3). In addition, a weaker luminescence band with longer wavelength at ~650 nm is discernible in Figure 7. This may be due to the excimer formation of *p*-TPAOXD, even though there is no evidence of excimer formation from the PL spectra. The device showed a sky blue luminescence at low applied voltage that turned to bluish white at elevated applied voltage because of the broadening of the EL spectra. The devices illustrated here started glowing with a turn-on voltage less than 8 V (Figure 8), which is comparable to or better than that for other single-layer devices based on bipolar light-emitting materials, which are mostly polymers.[16] The luminescence curve followed the current density curve closely, indicating equally efficient charge injection and transport processes for both electrons and holes for such single-layer devices. For a single-layer and blue light-emitting

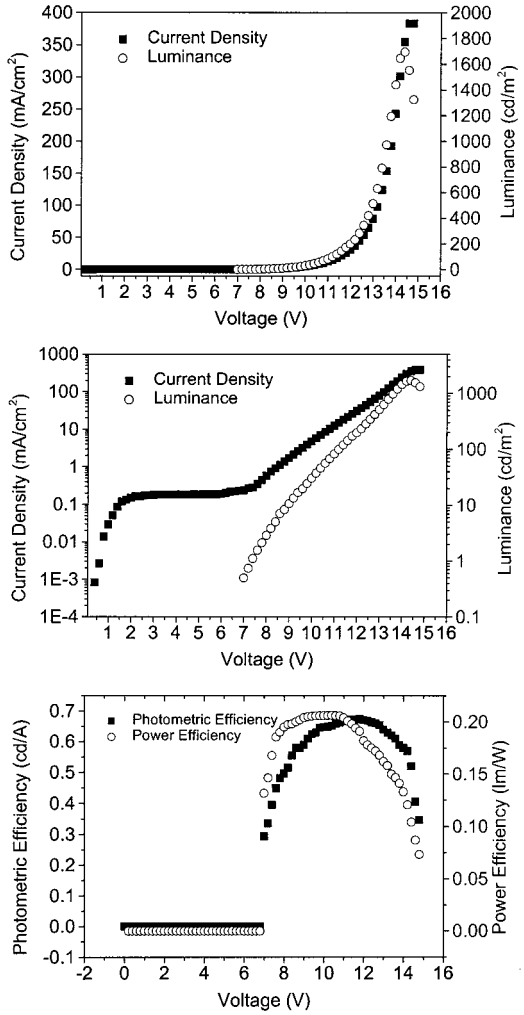

Figure 8. $I-V-L$ characteristics of the device ITO/*p*-TPAOXD (THF, 1000 Å)/Ca/Ag shown as double-linear plot (top) and a double-logarithmic plot (center) as well as the efficiency of the device (bottom).

device, this balanced charges behavior offers a relatively good power efficiency (~0.2 lm/W) or photometric efficiency (~0.7 cd/A) at a current density of ~10 mA/cm^2 (Figure 8). The device had a rather low current resistance by showing a current density higher than 350 mA/cm^2 (at 14.5 V) with little discernible decay. The brightness of the device can reach a maximum of 1690 cd/cm^2 under a driving voltage of ~14 V.

Different solvents (THF and cyclohexanone) used in spin-casting film formation did not generate much difference in performance such as current density, brightness, and efficiency. However, it is observed that devices fabricated using cyclohexanone always constantly have lower turn-on voltages (4−5 V) when compared to devices cast from THF (7−8 V) (Figures 8 and 9). We attribute this difference to the different viscosities and volatilities of the two solvents. The more viscous and less volatile cyclohexanone presumably promotes the formation of a homogeneous thin film by a spin-casting method.

(16) (a) Kido, J.; Harada, G.; Nagai, K. *Chem. Lett.* **1996**, 161. (b) Peng, Z.; Bao, Z.; Galvin, M. E. *Adv. Mater.* **1998**, *10*, 680. (c) Peng, Z.; Bao, Z.; Galvin, M. E. *Chem. Mater.* **1998**, *10*, 2086. (d) Liu, Y.; Ma, H.; Jen, A. K.-Y. *Chem. Commun.* **1998**, 2747. (e) Li, X.-C.; Liu, Y.; Liu, M. S.; Jen, A. K.-Y. *Chem. Mater.* **1999**, *11*, 1568.

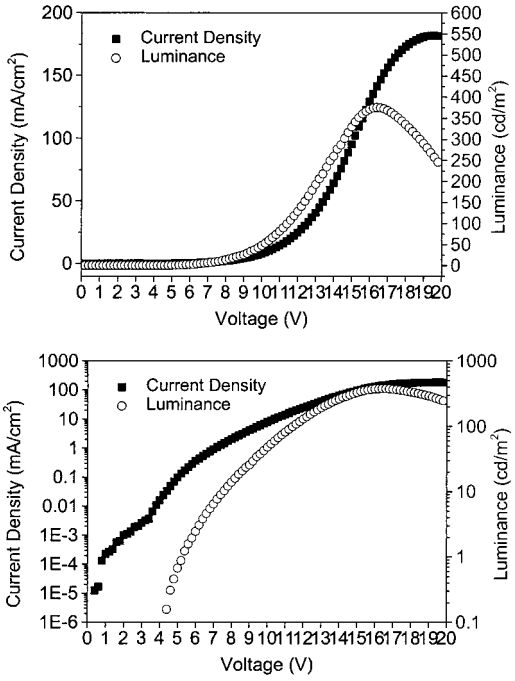

Figure 9. *I*−*V*−*L* characteristics of the device ITO/*p*-TPAOXD (cyclohexanone, 1200 Å)/Ca/Ag shown as a double-linear plot (top) and a double-logarithmic plot.

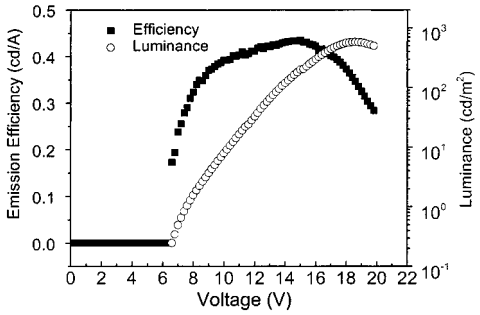

Figure 10. Efficiency−voltage−luminance characteristics of the device ITO/*p*-TPAOXD (THF, 1200 Å)/Ca/Ag.

It is noted that the EL spectra of the devices get narrower by replacing Ca/Ag with a LiF (∼10 Å)/Al cathode (Figure 7). The band narrowing is more apparent at the low-energy side of the emission, suggesting the possible formation of excimer or exciplex is somewhat inhibited due to the different cathode materials. The same phenomenon was also observed for devices based on *m*-TPAOXD.

The thickness of the light-emitting layer is a key factor that strongly affects the efficiency and luminance of the device. It is consistently observed that the device with a thick light-emitting layer (1200 Å) is less efficient and less bright than a device with a thinner layer (1000 Å) (Figure 10). A thinner emitting layer gives a better result but is also harder to fabricate by a spin-casting method.

Since the bipolar molecular material *p*-TPAOXD behaves more like an electron-transporting (or hole-blocking) material, a blending system containing both *p*-TPAOXD and hole-transporting PVK might provide a more efficient device. Figure 11 reveals that the device containing a 3:1 weight ratio blending of *p*-TPAOXD and PVK as the emitting layer has an enhanced photometric efficiency compared to that in Figure 8. The device can reach a maximum efficiency of 0.8 cd/A around 15 V with a current density less than 8 mA/cm^2. Although the efficiency improvement is modest and at the expense of device luminescence, the *p*-TPAOXD thin films are easier to spin-cast with the blending of PVK. A thinner single-layer device may be obtained with regained or further enhanced performance.

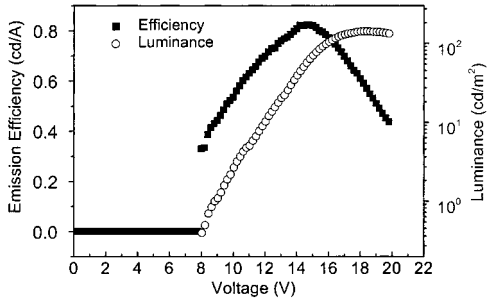

Figure 11. Efficiency−voltage−luminance characteristics of the device ITO/*p*-TPAOXD:PVK (3:1, cyclohexanone, 1200 Å)/Ca/Ag.

Finally, single-layer molecular devices with amorphous *m*-TPAOXD were also fabricated. The *I*−*V*−*L* characteristics studied reveal that current density is somewhat smaller, but the luminance of the devices containing *m*-TPAOXD is low (always less than 200 cd/m^2) and is about 8 to 10 times weaker than that for devices containing *p*-TPAOXD. This may be attributed to the much smaller ϕ_f of *m*-TPAOXD. Therefore, devices containing *m*-TPAOXD are usually less than half as efficient as those containing *p*-TPAOXD.

To conclude, we have demonstrated that 4-fold symmetrical tetraphenylmethane is an effective structural skeleton for improving thermal properties, that is, high melting temperature and stable glass phase, of compounds. Two bipolar isomers, *p*-TPAOXD and *m*-TPAOXD, are amorphous molecular materials with high T_g's of ∼190 and 150 °C, respectively. With judicious selection of the peripheral substituents, the tetraphenylmethane derivatives either serving as hole-blocking or light-emitting materials for OLED fabrication have been illustrated. The hole-blocking property of the oxadiazole-containing tetraphenylmethane CF3OXD was investigated and compared with that of PBD. We have examined the *I*−*V*−*L* characteristics and the efficiency of single-layer devices based on bipolar *p*-TPAOXD. Effects of parameters, such as solvent in spin-casting, material for the cathode, thickness of the film, and hole-transporting polymer blending, on performance were examined to provide a lead to device optimization.

Acknowledgment. This research was supported by the Chinese Petroleum Cooperation of the Republic of China.

CM0008056